Designing Ultrathin Film Composite Membranes: Importance of a Gutter Layer

Moon Kattula[1], Koushik Ponnuru[1], Ioannis Karampelas, Lingxiang Zhu[1], Weiguang Jia[1], Ting Wang[1] Haiqing Lin[1] and Edward P. Furlani[1, 2]

Dept. of Chemical & Biological Engineering[1], Dept. of Electrical Engineering[2],
University at Buffalo (SUNY), Buffalo, NY 14260-4200, efurlani@buffalo.edu

ABSTRACT

The performance of composite membranes that utilize an ultra-thin selective layer (<100 nm) can be improved with the introduction of an intermediate gutter layer (<100 nm) positioned between the selective layer and porous support. The properties of the gutter layer can be carefully chosen to enhance overall membrane performance, i.e., high permeance and high selectivity. However, the experimental determination of optimum gutter layer properties is very challenging, if not impossible, and modeling is needed to guide the selection process. In this presentation we address this need using a computational model to determine the effects of the gutter layer thickness and permeability on membrane performance. We show that a layer thickness of 1-2 times of the pore radius of the porous support yields the maximum improvement in permeance without significantly decreasing selectivity.

Keywords: thin film membrane, membrane design, gutter layer, permeance, selectivity, computational model.

1 INTRODUCTION

Membrane technology has been widely used for water purification, gas separation and has recently emerged as the leading technology for seawater desalination, nitrogen enrichment from air and CO_2 removal from natural gas.

Figure 1a shows a schematic of a thin film composite membrane for gas separation [1]. The thin, dense polymer layer (< 100 nm) performs molecular separation and the bulk porous support (150-200 μm) provides mechanical strength with negligible mass transport resistance. The porous support has small pores (< 100 nm) on the surface providing a smooth surface for the deposition of the selective layer [1,3,7]. However, as shown in Fig. 1b, this imposes a geometric restriction and increases the effective diffusion length (red lines) for penetrants, which decreases membrane performance and leads to a non-linear concentration profile of penetrants [4]. The effect of the support surface morphology on penetrant permeance has been studied using analytical models [5] as well as numerical models that precisely describe the concentration profile and flux within the selective layer for a given pore geometry.

To mitigate the geometric restriction derived from the porous support, a gutter layer with higher permeance than the selective layer can be used as an intermediate layer in practical membranes, as shown in Fig. 1b [5]. The gutter layer is made of extremely high permeability but low selectivity material (PTMSP & PDMS). Due to the high permeance, the gutter layer channels the permeate into the surface pores, reducing the geometric restriction without adding significant transport resistance [5]. In this presentation we use a computational model to elucidate the effect of the membrane nanofeatures on its separation performance.

2 THEORY AND MODELING

The support layer is assumed to contain a 2D array of uniformly spaced cylindrical pores. We can exploit the symmetry of this ordered pore structure and reduce the analysis to a unit cell of the membrane as shown in Fig. 2. Symmetry boundary conditions are applied on the sides of the unit cell to account for the surrounding membrane structure. The penetrant transport in the selective and gutter layers is diffusive and driven by the gradient in concentration following the solution-diffusion model. The equation that governs the steady-state concentration (CA) of a penetrant A in the membrane is [2],

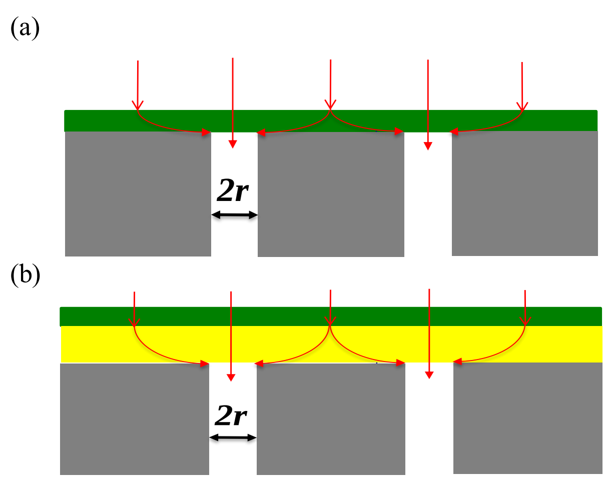

Fig.1 Schematics of thin film composite membrane: (a) a conventional two-layer thin film membrane comprised of a selective layer (with a thickness of l_s) on top of a porous support; (b) a three-layer composite membrane with an intermediate gutter layer of a thickness of l_g. The support has a pore radius of r.

$$\frac{\partial^2 C_A}{x^2} + \frac{\partial^2 C_A}{y^2} + \frac{\partial^2 C_A}{z^2} = 0 \tag{1}$$

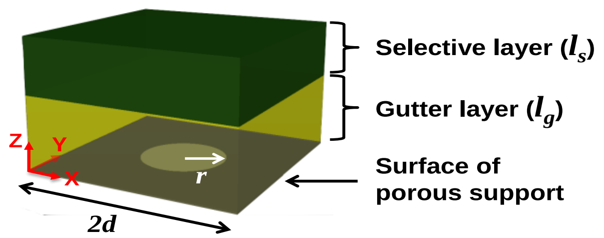

Fig 2. Schematic of a cubic unit cell: *2d*: unit cell length, *r* pore radius of the porous support.

The penetrant concentration and its flux are assumed to be continuous at the interface between the selective and gutter layers [2].

$$D_{A,g} \left. \frac{\partial C_{A,g}}{\partial z} \right|_{z=l_g} = D_{A,s} \left. \frac{\partial C_{A,s}}{\partial z} \right|_{z=l_g} \tag{2}$$

where D_A is the diffusion coefficient for penetrant A, and the subscripts of *s* and *g* indicate the selective and gutter layers, respectively. The nonporous region of the porous support is assumed to be impermeable and there is also zero-flux of the penetrant in the *x* and *y* direction through the sides of the unit cell because symmetry conditions are imposed at these boundaries.

The numerical model was implemented in the COMSOL multiphysics program (www.comsol.com), which solves the governing differential equations using the finite element method (FEM). An adaptive mesh function was used to ensure adequate refining of the mesh in the regions where the boundary condition transitions from a constant concentration to a no-flux condition. This has previously been shown to cause significant errors in the computation; therefore, refinement was continued until the calculated solution became mesh-independent.

The computational model predicts the concentration profile in the selective and gutter layers, and the resulting flux across the composite membrane. The geometric restriction of the membrane nanostructures on the observed permeance of penetrant A can be characterized as membrane permeance efficiency, β_A:

$$\beta_A = \frac{(P_A/l)_{Apparent}}{(P_A/l)_{Ideal}} \tag{3}$$

where $(P_A/l)_{Apparent}$ is the membrane permeance modeled, and $(P_A/l)_{Ideal}$ is the ideal permeance of the selective layer without the influence of the gutter layer and porous support (*i.e.*, $l_g = 0$ and $\phi = 1$). Lower β_A values indicate greater deviation from the ideal permeance, reflecting more severe effect from the porous support and/or the gutter layer.

3 RESULTS AND DISCUSSION

The simulation results depend on the porosity $\phi = \pi r^2/(4d^2)$ and the scaled selective layer thickness, $S = l_s/r$, and scaled gutter layer thickness, $G = l_g/r$, but not the absolute value of l_s or r [2,4]. In addition to the typical porosity values ranging from 0.01 to 0.1 [2,3] a porosity as high as 0.2 is also investigated in this work to explore the maximal benefits attainable by increasing the porosity. As shown in Fig. 3a, increasing porosity increases the membrane permeance efficiency. At a support porosity of 0.05 and a scaled selective layer thickness of 2, the permeance efficiency is as low as 0.17, indicating a significant flux restriction imposed by the porous support. These results are also consistent with those simulated for water transport by Ramon and coauthors, as represented as circles in Fig. 3a [2].

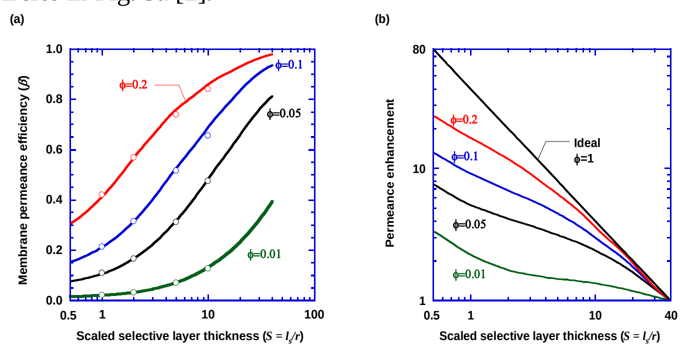

Fig. 3. Effect of the porous support porosity and the scaled selective layer thickness on (a) the membrane permeance efficiency (circles represent validation data taken from reference [2]) and (b) permeance enhancement.

Decreasing the selective layer thickness increases the ideal permeance, which, however, also decreases the permeance efficiency. Fig. 3b illustrates the compromised benefits of decreasing the selective layer thickness as a function of porosity (ϕ). However, due to the geometric restriction of the porous support, the permeance enhancement at *S* = 0.5 (ratio of apparent permeance at *S* = 0.5 to that at *S* = 40) is only 3.6, 7.6, and 13 at $\phi = 0.01$, 0.05, and 0.1, respectively. Even for a hypothetical porous support with $\phi = 0.2$, the expected 80 times increase in the ideal permeance yields only 25 times increase in the apparent permeance.

As shown in Fig. 1b, a gutter layer with negligible mass transfer resistance can channel the gas flow and thus mitigate geometric restriction by the porous support in the ultrathin film composite membranes. Figures 4a, 4b show that the streamlines along with the concentration profile which

TechConnect Briefs 2015, TechConnect.org, ISBN 978-1-4987-4728-8

represent diffusive paths through the selective and gutter layers. The pores increase the path length of the molecular transport and hence decrease the permeance. The increase in the path length is diminished with increasing porosity. Since the restriction is near the pore regions, it is expected that increasing the thickness of the selective layer and/or the gutter layer would minimize the pore restriction, and increase the concentration distribution in these layers.

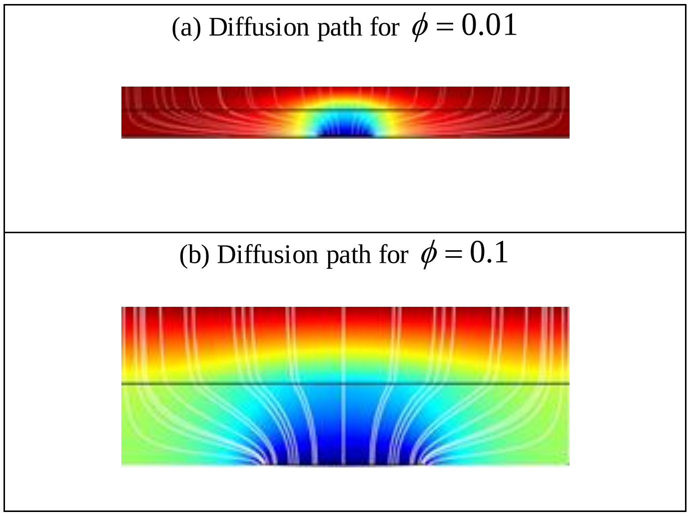

Fig. 4 Cutaway view of the 3D model unit cell showing the streamlines along with the concentration profile which represent diffusive paths through the selective and gutter layers for (a) $\phi = 0.01$ and (b) $\phi = 0.1$. In these calculations, $S = G = 1$; $P_g/P_s = 10$.

The gutter layer is assumed to have 10 times of permeability of the selective layer. The introduction of a gutter layer significantly increases permeance efficiency, though adding the gutter layer is expected to increase the mass transport resistance. As shown in the curves for membrane permeance efficiency (β) in Fig. 5a, introducing a thin gutter layer can increase the β value from 0.022 to as high as 0.13 (~ 6-fold increase) at ϕ = 0.01, and from 0.13 to 0.59 (~ 4.5-fold increase) at ϕ = 0.1. Figure 5a also shows the membrane permeance efficiency for overall selective and gutter layers ($\beta_A^{'}$), which is defined as the apparent permeance to the ideal permeance of the combined selective and gutter layer.

$$\beta_A^{'} = \frac{(P_A/l)_{Apparent}}{(P_A/l)_{Ideal,s+g}} = (P_A/l)_{Apparent}\left[\left(\frac{l}{P_A}\right)_s + \left(\frac{l}{P_A}\right)_g\right] = \beta_A + \frac{(P_A/l)_{Apparent}}{(P_A/l)_g} \quad (4)$$

where the subscripts of s, g, $s+g$ indicate the permeances for the selective layer only, gutter layer only, and the combined selective and gutter layer, respectively. Clearly, increasing the gutter layer thickness reduces the geometric restriction and thereby increases the β_A' values. On the other hand, further increase in the gutter layer thickness increases mass transport resistance in the gutter layer and thus decreasing the membrane permeance. Therefore, the benefit of reduced geometric restriction by the thicker gutter layer can be diminished by the increased mass transport resistance.

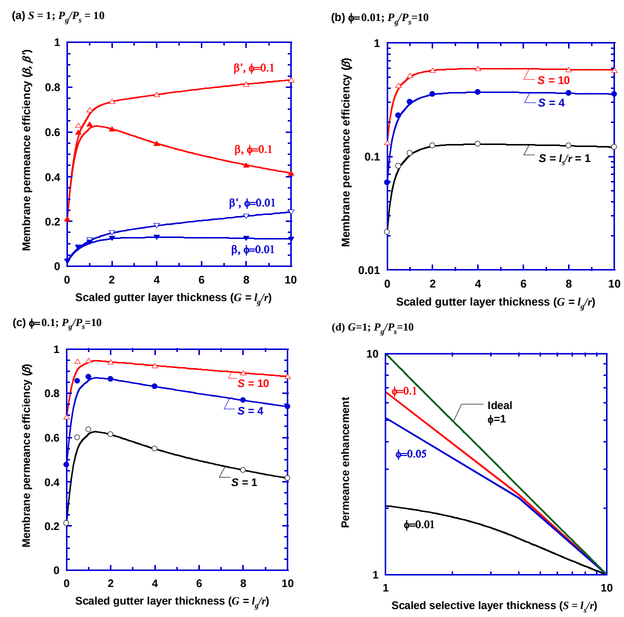

Fig. 5 Effect of the scaled gutter layer thickness G on (a) membrane permeance efficiency β_A and $\beta_A^{'}$ (defined as the ratio of the apparent permeance to the combined selective and gutter layer); (b) ϕ=0.01; (c) ϕ=0.1, and (d) permeance enhancement by decreasing selective layer thickness at G = 1 and various porosities. In all simulations, the permeability of the gutter layer is ten times that of the selective layer.

Figures 5b,c shows the quantitative effect of the gutter layer on membrane permeance efficiency at the scaled selective layer thicknesses ranging from 1 to 10, and porosity ϕ of 0.01 and 0.1. For these conditions, there seems to be an optimal gutter layer thickness of G between 1 and 2 to achieve the highest increase in permeance efficiency for various S values. Increasing the selective layer thickness increases the permeance efficiency, which is consistent to the study of two-layer composite membranes, as shown in Fig. 3. The most benefit of introducing the gutter layer is observed for the membranes with low porosity and thin selective layer, where the geometric restriction is most severe. Figure 5 also illustrates the importance of the porous supports. At ϕ =0.01, the best membrane permeance efficiency that can be achieved is 0.12 for S = 1, and 0.58 for S = 10. On the other hand, at $\phi = 0.1$, the greatest permeance efficiency achievable is 0.64 for S = 1, and 0.94 for S = 10. Therefore, porous supports with finer pores (lower r values and hence higher S values) and higher porosity are preferred. However, higher porosity may lead to the pore penetration of the coating solution during the membrane preparation, which blocks the pores and increases the support transport resistance, and thus decrease the membrane permeance [5]. Consequently, most commercial porous supports may have porosity less than 0.1. There remains a great challenge in producing the porous support with the balanced characteristics needed for membrane formation.

Figure 5d illustrates the benefit of decreasing the selective layer thickness at different porosities. The condition of $G = 1$ is chosen here for illustration, because it provides one of the greatest permeance efficiency values. While decreasing the selective layer thickness from $S = 10$ to $S = 1$ increases the ideal permeance by 10 times, the enhancement in apparent permeance is only 2.0 at $\phi = 0.01$, and 6.7 at $\phi = 0.1$. To put this on perspective, without the gutter layer, the permeance enhancement is only 1.5 at $\phi = 0.01$, and 5.1 at $\phi = 0.1$, though the permeance efficiency is much lower for the two-layer membranes compared to the three-layer membranes with the gutter layer, as shown in Fig. 5a. The results strongly indicate that the porous support and gutter layer are critical to designing high flux ultrathin membranes.

4 CONCLUSION

We have introduced a 3D computational model for predicting the performance of ultra-thin membranes and have used it to study the effect of an intermediate gutter layer on separation performance. The analysis shows that a gutter layer can be used to achieve high permeance, but it can decrease the selectivity when the porous support has low porosity. A gutter layer thickness of 1-2 times the pore radius of the porous support yields the maximum improvement in the membrane permeance without significantly decreasing selectivity. The model is readily implemented in commercially avaiable software and enable the rational design of ultrathin composite membranes.

REFERENCES

[1] R.W. Baker, Membrane Technology and Applications, 3rd ed., John Wiley and Sons, Ltd., Chichester, UK, 2012.
[2] G.Z. Ramon, M.C.Y. Wong, E.M.V. Hoek, Transport through composite membrane, part 1: Is there an optimal support membrane?, J. Membr. Sci., 415 (2012) 298-305.
[3] X. Lu, L. H. Arias Chavez, S. Romero-Vargas Castrillón, J. Ma and M. Elimelech, Environ. Sci. Techn., 2015, In press.
[4] H. K. Lonsdale, R. L. Riley, C. R. Lyons and D. P. Carosella, in Membrane Processes in Industry and Biomedicine, ed. M. Bier, Plenum Press, New York, 1971, pp. 101-122.
[5] K.A. Lundy, I. Cabasso, Analysis and construction of multilayer composite membranes for the separation of gas mixtures, Ind. Eng. Chem. Res., 28 (1989) 742-756.
[6] T. C. Merkel, H. Lin, X. Wei and R. W. Baker, J. Membr. Sci., 2010, 359, 126-139.
[7] H. Lin, M. Zhou, J. Ly, J. Vu, J. G. Wijmans, T. C. Merkel, J. Jin, A. Haldeman, E. H. Wagener and D. Rue, Ind. Eng. Chem. Res., 2013, 52, 10820-10834.